SCIENCE CHINA
Technological Sciences

•Article•

November 2023 Vol.66 No.11: 3309–3316
https://doi.org/10.1007/s11431-022-2361-8

Influence of oscillation strain on the dynamic mechanical relaxation of a La-based metallic glass

LIANG ShuYi[1], ZHANG LangTing[1], WANG YunJiang[2,3], PINEDA E.[4] & QIAO JiChao[1,5*]

[1] *School of Mechanics, Civil Engineering and Architecture, Northwestern Polytechnical University, Xi'an 710072, China;*
[2] *State Key Laboratory of Nonlinear Mechanics, Institute of Mechanics, Chinese Academy of Sciences, Beijing 100190, China;*
[3] *School of Engineering Science, University of Chinese Academy of Sciences, Beijing 100049, China;*
[4] *Department of Physics, Institute of Energy Technologies, Universitat Politècnica de Catalunya – BarcelonaTech, Barcelona 08019, Spain;*
[5] *Innovation Center, NPU-Chongqing, Chongqing 401135, China*

Received December 17, 2022; accepted February 21, 2023; published online June 26, 2023

Dynamic mechanical relaxation processes, particularly secondary relaxation processes, are closely related to the mechanical and physical properties of metallic glasses. Here the effect of oscillation strain amplitude on the secondary relaxation of a typical La-based metallic glass was studied using the dynamic mechanical analysis method. The apparent activation energy of the β relaxation is shown to increase with the oscillation strain amplitude. When it changes from 0.02% to 0.16%, the activation energy increases from 0.73 to 0.96 eV. Simultaneously, the intensity of the β relaxation shifts toward high temperature. Additionally, the apparent β relaxation is found to be sensitive to the physical aging below the glass transition temperature. The findings suggest a correlation between the inelastic deformation and the relaxation behavior of amorphous metals.

metallic glass, dynamic mechanical analysis, internal friction, β relaxation, oscillation amplitude

Citation: Liang S Y, Zhang L T, Wang Y J, et al. Influence of oscillation strain on the dynamic mechanical relaxation of a La-based metallic glass. Sci China Tech Sci, 2023, 66: 3309–3316, https://doi.org/10.1007/s11431-022-2361-8

1 Introduction

Metallic glasses (MGs) are solids with disordered atomic structures. They belong to a new type of material within the broad family of glasses. Because of this unique structural feature, MGs show promising mechanical/physical properties compared with their crystalline counterparts [1–8]. It is well known that crystalline "Defects" (i.e., vacancies, interstitials, dislocations, and grain boundaries) control the mechanical and physical properties of the traditional metallic materials. However, understanding the link between the mechanical properties and microstructure of MGs remains a challenging issue in both condensed matter physics and materials science [9–12].

Usually, two major relaxation processes occur in the glassy materials, namely, the primary relaxation (α relaxation process) and the secondary relaxation (β relaxation process) [13,14]. The α relaxation process of amorphous materials is generally accepted as a large-scale and irreversible rearrangement of atoms or molecules, which is related to the glass transition phenomenon [15,16]. Conversely, the β relaxation process corresponds to the local movement of atoms or molecules [17]. Unlike the α relaxation process, β relaxation is the principal carrier of dynamics in the glassy state, as relaxation freezes below the glass transition temperature T_g [18–21]. The relaxation processes are the key to the understanding of the diffusion behavior, mechanical properties (i.e., plasticity), and glass transition phenomenon of the general amorphous materials [3,6,22–27].

Previous investigations have proven that the β relaxation process of MGs is sensitive to its chemical composition [28,29], thermal treatment (i.e., physical aging) [30,31],

* Corresponding author (email: qjczy@nwpu.edu.cn)

plastic deformation (e.g., cold rolling [32–34]), mechanical milling [35], and thermomechanical cyclic treatments [36,37]. A highly stable glassy state can be attained via physical aging below the glass transition temperature, and this process reduces the atomic mobility and slows the dynamics of glass [38,39]. The atomic hopping rate and the propensity of cooperative rearrangements are governed by the magnitude of activation energy. The atomic mobility decreases when the activation energy increases [40,41]. Moreover, the activation volume of the flow defects is also important in understanding the atomic or molecular motion of the glassy materials and their dynamic relaxations [42–44]. Elastostatic loading imposed on an MG introduces structural heterogeneity that is associated with structural shear and dilatation at both short- and medium-range atomic scales. It is also connected to the concentration of free volume in a glass sample [45]. For example, by modulating the amplitude and time of ultrasonic vibration, the ductility of MG composites can be improved owing to their unique softening behavior [46].

Based on such observations, the structural evolution of an amorphous alloy must be experimentally probed, in order to link structure to the β relaxation. This paper attempts to offer new physical insight into the structural evolution behavior of a prototypical $La_{62}Al_{14}Ag_{2.34}Ni_{10.38}Co_{10.38}$ MG, a material that is featured with a pronounced β relaxation process, through strain oscillation loading with different amplitudes.

2 Experimental procedure

2.1 Sample preparation

A $La_{62}Al_{14}Ag_{2.34}Ni_{10.38}Co_{10.38}$ MG was chosen as a model alloy system, as it shows excellent glass-forming ability [47] and pronounced β relaxation character. Master alloy ingots were prepared via arc melting under an argon atmosphere. The ingot has been remelted five times to ensure chemical homogeneity. Plates with dimensions of 70 mm (length), 10 mm (width), and 2 mm (thickness) were prepared using a copper mold suction casting technique. The glass nature of the model alloy was verified by the X-ray diffraction pattern (XRD, X'Pert PRO). The broad diffraction peak confirms the amorphous state of the alloy (as shown in the inset of Figure 1). The thermal properties of the model alloy were measured using differential scanning calorimetry (DSC) (Netzsch DSC404). In Figure 1, the DSC curve of the La-based MG indicates that the glass transition temperature T_g~443 K. The onset temperature of crystallization is determined as 473 K.

2.2 Dynamic mechanical analysis

The dynamic mechanical behavior of the La-based MG was investigated using the dynamic mechanical analysis (DMA) in a commercial TA-instruments Q850 apparatus in single cantilever bending mode. The dimensions of the samples were 30 mm (length), 2 mm (width), and 1 mm (thickness). When a sinusoidal stress is applied to the sample, the strain is measured, providing information about the change in its mechanical properties with temperature. The strain over time can be written as follows:

$$\gamma(t) = \gamma_0 \sin(\omega t), \tag{1}$$

where γ_0 is the driving strain amplitude of oscillation and ω is the angular frequency. Because viscoelasticity is intrinsic in amorphous solids, the corresponding stress exhibits a phase lag angle θ with respect to strain. The former is expressed as follows:

$$\tau(t) = \tau_0 \sin(\omega t + \theta), \tag{2}$$

where τ_0 is the stress amplitude. The complex modulus of materials is defined as follows:

$$\begin{aligned} E &= \frac{\tau(t)}{\gamma(t)} = \frac{\tau_0}{\gamma_0}\exp(\mathrm{i}\theta) \\ &= \frac{\tau_0}{\gamma_0}(\cos\theta + \mathrm{i}\sin\theta) = E' + \mathrm{i}E'', \\ E' &= \frac{\tau_0}{\gamma_0}\cos\theta, \\ E'' &= \frac{\tau_0}{\gamma_0}\sin\theta, \end{aligned} \tag{3}$$

where E' is the storage modulus, which determines the stored elastic energy during deformation. E'' is the loss modulus describing the loss of energy transformed into heat because of the viscous contribution. The relation between strain and stress shows a stable hysteresis loop whose area is equal to the dissipated energy, ΔW, lost as heat during one oscillation cycle. The internal friction $\tan\delta = E''/E'$, which is closely correlated with ΔW. The internal friction is generally used to describe the damping behavior of materials. In the case of amorphous solids, internal friction is closely related to the movement of atoms or molecules.

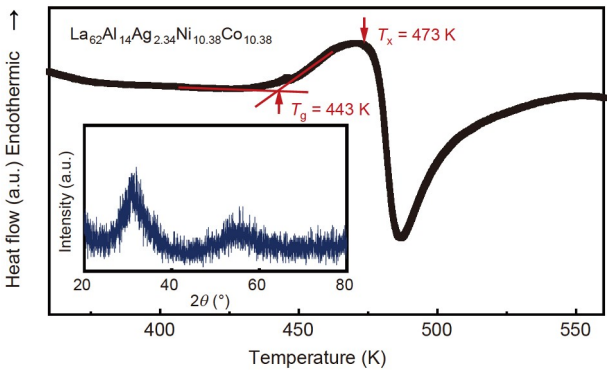

Figure 1 (Color online) DSC curve of the $La_{62}Al_{14}Ag_{2.34}Ni_{10.38}Co_{10.38}$ MG (the heating rate is 20 K/min). The inset is the XRD pattern of the $La_{62}Al_{14}Ag_{2.34}Ni_{10.38}Co_{10.38}$ MG.

3 Results and discussion

3.1 Dynamic mechanical relaxation behaviors

The evolution of the normalized storage modulus and the loss modulus of the La-based MG with temperature can be divided into three typical regions, as shown in Figure 2, for the case of heating rate of 1 K/min and a driving frequency of 3 Hz. Region I: At low temperatures (from room temperature to 370 K), E'/E_u is high and nearly constant, while the viscoelastic component E''/E_u is very low. In this temperature region, the mechanical behavior of MG is dominated by elastic deformation. However, when the temperature reaches ~340 K, a prominent β relaxation peak can be observed. Unlike the La-based MGs, Zr-based MGs usually show an excess wing in the relaxation curve instead of a pronounced secondary relaxation. This behavior is clearly shown in Figure 3. Region II: The loss modulus reaches its maximum peak at ~448 K. This location is corresponding to the primary or α relaxation process. The α relaxation corresponds to the dynamic glass transition phenomenon, which is linked to the collective motion of atoms or molecules. Region III: Because of the onset of crystallization, the storage modulus increases and the loss modulus decreases with increasing temperature [48].

3.2 Effect of oscillation amplitude on β relaxation

Figure 4(a) shows the evolution of the normalized loss modulus E''/E_u of the La-based MG as a function of temperature for different driving frequencies (0.5, 1, 2, 4, 8, and 16 Hz) when the strain amplitude of oscillation is 0.08%. The peak temperature of the β relaxation T_β shifts to higher temperature, and its intensity increases with increasing driving frequency. The correlation between T_β and the driving frequency obeys the Arrhenius equation, which is expressed as follows [49]:

$$f = f_0 \exp\left(-\frac{E_\beta}{k_B T_\beta}\right), \tag{4}$$

where f is the driving frequency, T_β is the absolute temperature at which β relaxation occurs, E_β is the apparent activation energy of the β relaxation process, k_B is Boltzmann's constant, and f_0 is a characteristic frequency. The activation energy of β relaxation was readily computed and shown in the inset of Figure 4(a). The dynamical features of the β relaxation process are depicted in Figure 4(b) when applying different strain amplitudes of oscillation. The peak temperature of the normalized modulus increases considerably with strain amplitude (0.02%, 0.04%, 0.08%, and 0.16%), and its intensity is enhanced when the strain amplitude increases. As shown in the inset of Figure 4(b), E_β

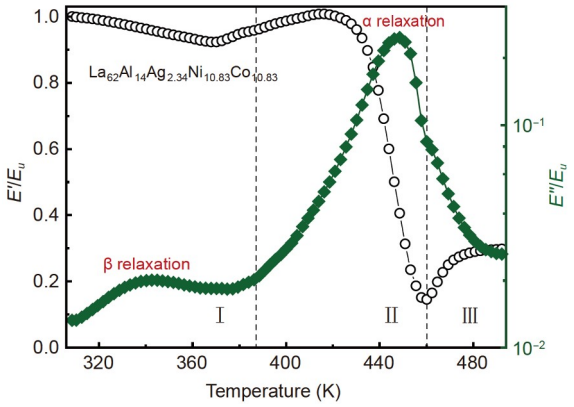

Figure 2 (Color online) Normalized storage modulus and loss modulus as a function of temperature. The β relaxation and α relaxation features are indicated by the peaks in the normalized loss modulus at approximately 340 K and 450 K, respectively.

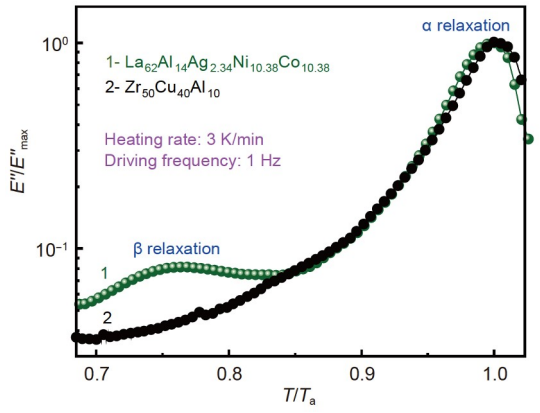

Figure 3 (Color online) Normalized loss modulus as a function of normalized temperature for La-based ($La_{62}Al_{14}Ag_{2.34}Ni_{10.38}Co_{10.38}$) and Zr-based ($Zr_{50}Cu_{40}Al_{10}$) MGs.

increases with increasing oscillation strain amplitude. Therefore, the hysteresis effect increases as strain amplitude increases. It implies that the internal friction gradually increases.

According to the cooperative shearing model proposed by Johnson and Samwer [50], the relation between the activation volume $V(T)$ and the activation energy E_{csm} of the elementary deformation unit in MGs is expressed as follows:

$$V(T) = \frac{E_{csm}}{\frac{8}{\pi^2} G(T) \xi \gamma_c^2}, \tag{5}$$

where $G(T)$ is the temperature-dependent elastic shear modulus. The critical strain is $\gamma_c \approx 0.027$, and the correction factor is $\xi \approx 3$. Considering that the Poisson ratio of the La-based MG $\nu \approx 0.32$ [6] and $E_{csm} \approx E_\beta$, the evolution of the shear modulus with temperature can be generally expressed as follows [19]:

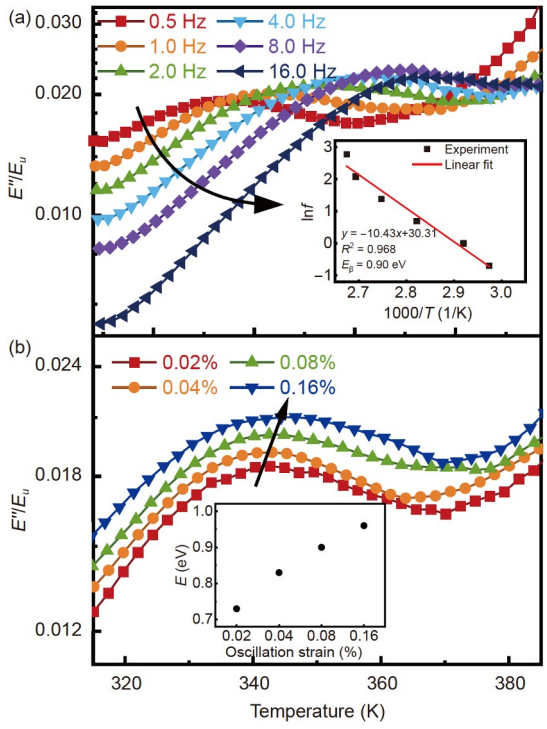

Figure 4 (Color online) (a) Normalized loss modulus as a function of temperature at different driving frequencies (0.5, 1.0, 2.0, 4.0, 8.0, and 16.0 Hz). The temperature window ranges from room temperature to 390 K. The inset shows an Arrhenius plot of the frequency *versus* temperature with an oscillation amplitude of 0.08% strain. The solid line is fit by eq. (4). (b) Evolution of the normalized loss modulus with temperature at various strain amplitude oscillations (0.02%, 0.04%, 0.08%, and 0.16%). The inset is the apparent activation energy of the β relaxation process at different oscillation strains.

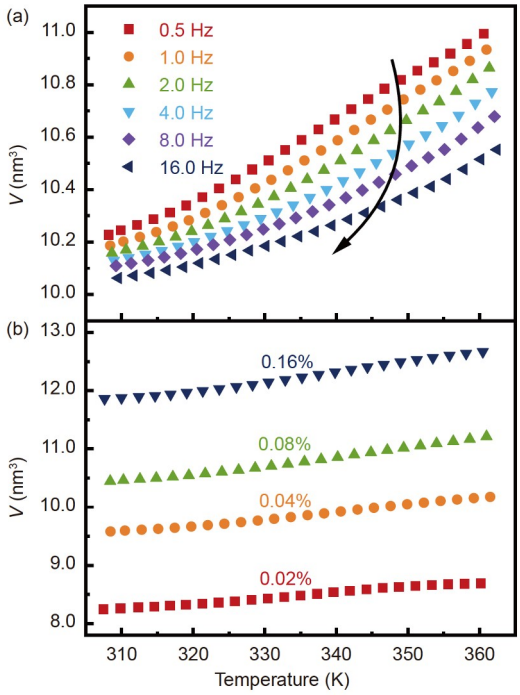

Figure 5 (Color online) (a) Flow defect volume as a function of temperature at different frequencies during the β process with an oscillation strain amplitude of 0.08%. (b) Flow defect volume as a function of temperature over different oscillation strain amplitudes at a frequency of 1 Hz in the range of β relaxation.

$$G(T)=\frac{E(T)}{2(1+\nu)}=\frac{(E'(T)^2+E''(T)^2)^{\frac{1}{2}}}{2(1+\nu)}. \tag{6}$$

The relation between the flow defect volume and temperature can be calculated, and it is depicted in Figure 5(a) and (b). Moreover, V decreases with increasing driving frequency, with a value between 10 and 11 nm^3. Additionally, the disparity in activation volumes corresponds to the difference in frequency. The activation volume is large when the temperature is high. The influence of the strain amplitude of oscillation on V is stronger compared with the effect of frequency in the entire temperature range of the β relaxation process. The activation volume increases when the oscillation strain increases from 0.02% to 0.16%. The characteristic relaxation time is closely related to the local atomic rearrangement of flow defects. The increase in driving frequency decreases the characteristic relaxation time. However, it increases the deformation applied to the material. Since the deformation is in the nonlinear region, so that it decreases the free energy barrier of β relaxation [51]. Because of the increase in the strain amplitude, the corresponding input energy also increases. This facilitates the local movement of atoms such that the activation volume of flow defect increases considerably.

3.3 Effect of the strain on the β relaxation process

Mechanical spectroscopy has been widely employed to extract the fundamental physical parameters of glasses, such as the storage modulus, loss modulus, and internal friction, guiding the exploration of the atomic rearrangement mechanism during the strain-assisted and thermally activated processes happens during dynamics of materials [2]. The loss modulus spectra can be well described by the Havriliak-Negami (HN) model with input of the β relaxation, which can be written as follows [52]:

$$G^*(\omega)=\frac{\Delta G_\beta}{(1+(\mathrm{i}\omega\tau_\beta)^m)^n}, \tag{7}$$

where ΔG_β is the relaxation strength, ω is the angular frequency, τ_β is the characteristic time of β relaxation, and m and n are shape parameters. The values of these two parameters vary from 0 to 1. Notably, when n=1, eq. (7) corresponds to the Cole-Cole equation. Figure 6(a) and (b) show the curves of the normalized loss modulus E''/E_u fitted by the HN model for the $La_{62}Al_{14}Ag_{2.34}Ni_{10.38}Co_{10.38}$ MG. As shown in Figure 6(a), when temperature increases, the peak of the β relaxation shifts toward high frequencies, and its

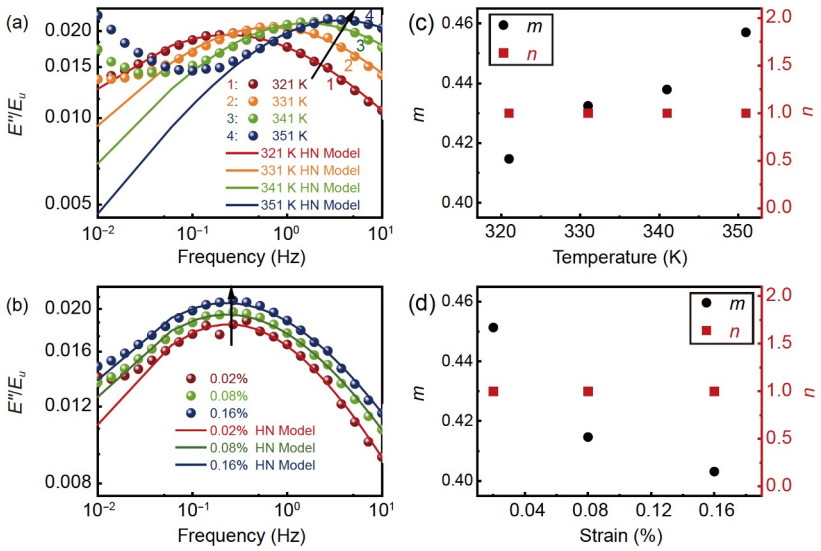

Figure 6 (Color online) (a) The frequency spectrum of the normalized loss modulus at different temperatures by DMA experiments. (b) Frequency spectrum over oscillations with different strain amplitudes. In (a) and (b), the solid lines denote the best fit by the HN model. (c), (d) Parameters *m* and *n* of the HN model as functions of temperature and strain amplitude, respectively.

intensity increases. Moreover, similar behavior is observed when the oscillation strain increases. Parameter *m*, representing the width of the relaxation spectrum, increases with temperature and decreases with the driving strain. Meanwhile, parameter *n*, representing the asymmetric character of the relaxation peak, remains constant at a value of 1, as shown in Figure 6(c) and (d). The product of the *m* and *n* parameters, *m***n*, demonstrates the structural features of an MG [53–56]. A small value of *m***n* usually indicates a high level of heterogeneity. As shown in Figure 6(c) and (d), increasing temperature increases the value of *m***n* in a given frequency range, illustrating that the structure of the La-based MG becomes increasingly homogeneous with increased temperature. Additionally, the structural heterogeneity increases when the oscillation strain increases from 0.02% to 0.16%.

The physical origin and evolution of the relaxation dynamics of MGs are closely connected with their structural heterogeneity [2]. Experimental and theoretical fittings demonstrate that the peak value of the loss modulus is positively correlated with the strain amplitude of oscillation during the β relaxation process. Upon intensifying the mechanical stimulus, the atomic mobility also increases, such that less time is required for the activation of the β relaxation process. Therefore, the β relaxation time τ_β decreases when the oscillation strain increases. When the oscillation strain increases from 0.02% to 0.16%, the structural heterogeneity increases, and the physical and mechanical properties show various degrees of changes. Therefore, the thermodynamic features of the MG used herein can be improved by manipulating the oscillation amplitude, even in the nominal elastic zone of such viscoelastic material.

3.4 Influence of the oscillation strain on the initial state of the MG

Physical aging is an important way of tuning the mechanical and physical properties of amorphous solids [30,31]. Figure 7(a) plots the normalized storage modulus and loss modulus of the La-based MG *versus* its physical aging time. The physical aging temperature is 380 K. The storage modulus increases while the loss modulus decreases when aging proceeds. The loss factor (or loss modulus) of the amorphous solids is closely connected to the movement of atoms or molecules. Physical aging decreases the atomic mobility in MGs. The evolution of the loss factor with annealing time can be well described based on the Kohlrausch-Williams-Watts (KWW) equation, expressed as follows [57]:

$$\tan\delta(t) = \tan\delta(t=0) - A\left\{1 - \exp\left[-\frac{t}{\tau}\right]^{\beta_{\mathrm{KWW}}}\right\}, \tag{8}$$

where A is the maximum magnitude of the relaxation, and τ is the characteristic time of the annealing process. β_{KWW} is the KWW exponential stretching parameter, which is correlated to the structural heterogeneity in MGs [58]. In this scenario, the effect of physical aging can be measured using DMA following the evolution of the parameter Δ defined as follows [57]:

$$\Delta(t) = \frac{\tan\delta(t) - \tan\delta(t=\infty)}{\tan\delta(t=0) - \tan\delta(t=\infty)}. \tag{9}$$

The inset of Figure 7(a) shows a double logarithmic plot of the loss factor tan*δ* *versus* the physical aging time. In addition, β_{KWW} depends on the oscillation strain applied during the isothermal process when other conditions are fixed. The various values of β_{KWW} (as shown in Figure 7(b)) also

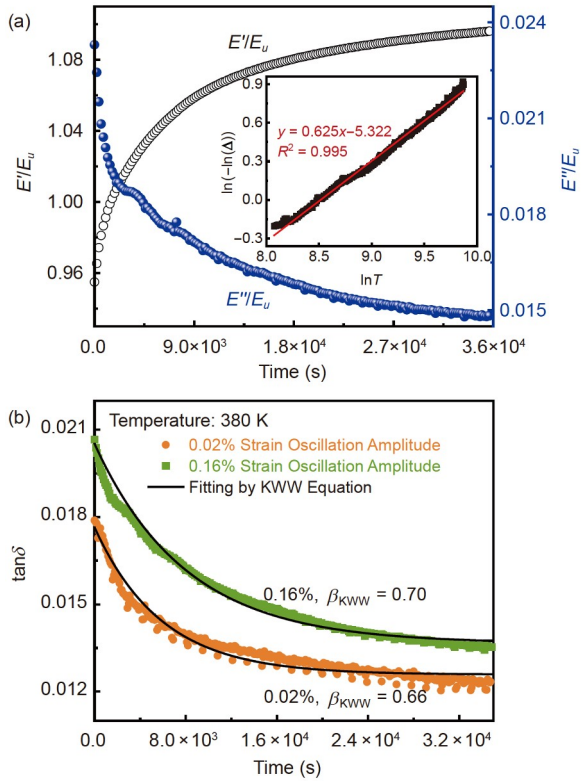

Figure 7 (Color online) (a) Dynamical behavior of $La_{62}Al_{14}Ag_{2.34}Ni_{10.38}Co_{10.38}$ MG during an isothermal procedure at a temperature of 380 K with an oscillation of strain amplitude of 0.16%. The inset displays the scaling between the loss factor tanδ and time. (b) Evolution of loss factor tanδ with isothermal time at various oscillation strain amplitudes, i.e., 0.02% and 0.16%.

indicate that the strain oscillation during annealing has a visible effect on its structural heterogeneity. Figure 8 compares the as-cast and annealed glass samples. When oscillations with various strain amplitudes (0.02%, 0.04%, 0.08%, and 0.16%) are imposed on the annealed MG, the β relaxation process clearly separates from the α relaxation process, in the case of oscillations with large strain. The peak temperature of the annealed samples is higher, and the intensity of its β relaxation is weaker compared with those of the as-cast samples under identical conditions, i.e., heating rate: 2 K/min, driving frequency: 1 Hz, and strain amplitude of oscillation: 0.08%.

When the strain amplitude of oscillation gradually increases, it accelerates the local atomic motion in MG. Moreover, this leads the MG to a relatively more stable thermodynamic state with larger activation energy for the dynamic processes. Even in the nominally elastic region, typical inelastic flow occurs, and the stress-strain hysteresis loops appear when the sinusoidal strain is applied to an amorphous alloy during the isothermal annealing process. With increasing strain amplitude, the activation volume of flow defects and the apparent activation energy show a substantial increase owing to the enhancement of structural relaxation. This process implies that the atomic motion in the

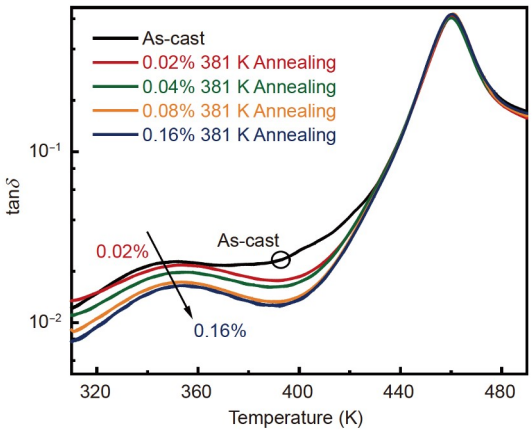

Figure 8 (Color online) Internal friction tanδ as a function of temperature for MGs under various initial conditions.

MG is restricted, and the microstructural homogeneity of the La-based MG is greatly improved. Moreover, even oscillation with a small strain amplitude would substantially affect the microscopic structure of the MG owing to the subtle changes over a long time.

4 Conclusion

In sum, we find that application of strain oscillation with different magnitudes on a La-based MG influences its β relaxation process. This nonlinear response to a mechanical perturbation is found for small strain amplitude within the nominally elastic region of MG. The increase in the oscillation strain injects substantial energy into the system. The apparent activation energy of the β relaxation process increases from 0.73 to 0.96 eV when the strain amplitude changes from 0.02% to 0.16%. This change also implies that the internal friction increases in this material. Additionally, the number of activated flow defects increases with increasing oscillation strain, or the frequency applied to the MG is increased. This observation is in accordance with the scenario of the cooperative shearing model. With increasing strain amplitude, the intensity of the β relaxation process is enhanced, and the β relaxation temperature approaches a higher value. Moreover, the DMA illustrates that different states are obtained by applying different strain amplitudes, when the annealing is also conducted below T_g. The oscillation strain also yields substantially different β relaxation behaviors, increases atomic mobility and drives MG to relatively a more stable thermodynamic state.

This work was supported by the National Natural Science Foundation of China (Grant Nos. 51971178 and 52271153), the Natural Science Basic Research Plan for Distinguished Young Scholars in Shaanxi Province (Grant No. 2021JC-12), and the Natural Science Foundation of Chongqing (Grant No. cstc2020jcyj-jqX0001). PINEDA E. acknowledges financial support from "Proyecto PID2020-112975GB-I00 de investigación fi-

nanciado por MCIN/AEI /10.13039/501100011033" and Generalitat de Catalunya AGAUR 2021-SGR-343 grant. WANG Yun-Jiang is supported by the National Natural Science Foundation of China (Grant No. 12072344) and the Youth Innovation Promotion Association of the Chinese Academy of Sciences.

1 Sheng H W, Luo W K, Alamgir F M, et al. Atomic packing and short-to-medium-range order in metallic glasses. Nature, 2006, 439: 419–425
2 Qiao J C, Wang Q, Pelletier J M, et al. Structural heterogeneities and mechanical behavior of amorphous alloys. Prog Mater Sci, 2019, 104: 250–329
3 Chang C, Zhang H P, Zhao R, et al. Liquid-like atoms in dense-packed solid glasses. Nat Mater, 2022, 21: 1240–1245
4 Johnson W. Thermodynamic and kinetic aspects of the crystal to glass transformation in metallic materials. Prog Mater Sci, 1986, 30: 81–134
5 Qiao J, Zhang L, Tong Y, et al. Mechancial properties of amorphous alloys: In the framework of the microstructure heterogeneity (in Chinese). Adv Mech, 2022, 52: 117–152
6 Wang W H. Dynamic relaxations and relaxation-property relationships in metallic glasses. Prog Mater Sci, 2019, 106: 100561
7 Yu H B, Shen X, Wang Z, et al. Tensile plasticity in metallic glasses with pronounced β relaxations. Phys Rev Lett, 2012, 108: 015504
8 Zhang L T, Duan Y J, Crespo D, et al. Dynamic mechanical relaxation and thermal creep of high-entropy $La_{30}Ce_{30}Ni_{10}Al_{20}Co_{10}$ bulk metallic glass. Sci China-Phys Mech Astron, 2021, 64: 296111
9 Wang W H, Dong C, Shek C H. Bulk metallic glasses. Mater Sci Eng-R-Rep, 2004, 44: 45–89
10 Schneider S. Bulk metallic glasses. J Phys-Condens Matter, 2001, 13: 7723–7736
11 Wagner H, Bedorf D, Küchemann S, et al. Local elastic properties of a metallic glass. Nat Mater, 2011, 10: 439–442
12 Lan S, Zhu L, Wu Z, et al. A medium-range structure motif linking amorphous and crystalline states. Nat Mater, 2021, 20: 1347–1352
13 Wang W H. The elastic properties, elastic models and elastic perspectives of metallic glasses. Prog Mater Sci, 2012, 57: 487–656
14 Wang Q, Zhang S T, Yang Y, et al. Unusual fast secondary relaxation in metallic glass. Nat Commun, 2015, 6: 7876
15 Hao Q, Lyu G J, Pineda E, et al. A hierarchically correlated flow defect model for metallic glass: Universal understanding of stress relaxation and creep. Int J Plast, 2022, 154: 103288
16 Yu H B, Wang W H, Bai H Y, et al. The β-relaxation in metallic glasses. Natl Sci Rev, 2014, 1: 429–461
17 Spieckermann F, Şopu D, Soprunyuk V, et al. Structure-dynamics relationships in cryogenically deformed bulk metallic glass. Nat Commun, 2022, 13: 127
18 Qiao J C, Wang Q, Crespo D, et al. Amorphous physics and materials: Secondary relaxation and dynamic heterogeneity in metallic glasses: A brief review. Chin Phys B, 2017, 26: 016402
19 Zhang L T, Wang Y J, Pineda E, et al. Achieving structural rejuvenation in metallic glass by modulating β relaxation intensity via easy-to-operate mechanical cycling. Int J Plast, 2022, 157: 103402
20 Johari G P, Goldstein M. Viscous liquids and the glass transition. II. Secondary relaxations in glasses of rigid molecules. J Chem Phys, 1970, 53: 2372–2388
21 Sun Y, Peng S X, Yang Q, et al. Predicting complex relaxation processes in metallic glass. Phys Rev Lett, 2019, 123: 105701
22 Yu H B, Wang W H, Samwer K. The β relaxation in metallic glasses: An overview. Mater Today, 2013, 16: 183–191
23 Wang Q, Liu J J, Ye Y F, et al. Universal secondary relaxation and unusual brittle-to-ductile transition in metallic glasses. Mater Today, 2017, 20: 293–300
24 Yang Q, Peng S X, Wang Z, et al. Shadow glass transition as a thermodynamic signature of β relaxation in hyper-quenched metallic glasses. Natl Sci Rev, 2020, 7: 1896–1905
25 Qiao J C, Liu X D, Wang Q, et al. Fast secondary relaxation and plasticity initiation in metallic glasses. Natl Sci Rev, 2018, 5: 616–618
26 Zhou Z Y, Sun Y, Gao L, et al. Fundamental links between shear transformation, β relaxation, and string-like motion in metallic glasses. Acta Mater, 2023, 246: 118701
27 Huang B, Yuan C C, Wang Z Q, et al. Influence of short- to medium-range electronic and atomic structure on secondary relaxations in metallic glasses. Acta Mater, 2020, 196: 88–100
28 Pei C Q, Xie J Y, Zhao Y, et al. Hidden and universal relaxation mode in metallic glasses of simple atomic structure. Phys Rev B, 2022, 106: 214203
29 Yu H B, Samwer K, Wang W H, et al. Chemical influence on β-relaxations and the formation of molecule-like metallic glasses. Nat Commun, 2013, 4: 2204
30 Casalini R, Roland C M. Aging of the secondary relaxation to probe structural relaxation in the glassy state. Phys Rev Lett, 2009, 102: 03570131
31 Giordano V M, Ruta B. Unveiling the structural arrangements responsible for the atomic dynamics in metallic glasses during physical aging. Nat Commun, 2016, 7: 10344
32 Qiao J C, Pelletier J M. Dynamic mechanical relaxation in bulk metallic glasses: A review. J Mater Sci Tech, 2014, 30: 523–545
33 Wang T, Wu Y D, Si J J, et al. Plasticizing and work hardening in phase separated Cu-Zr-Al-Nb bulk metallic glasses by deformation induced nanocrystallization. Mater Des, 2018, 142: 74–82
34 Johnson W L. Bulk glass-forming metallic alloys: Science and technology. MRS Bull, 1999, 24: 42–56
35 Li X X, Wang J G, Ke H B, et al. Extreme rejuvenation and superior stability in a metallic glass. Mater Today Phys, 2022, 27: 100782
36 Stringe M, Spangenberg K, da Silva Pinto M W, et al. Decoupled alpha and beta relaxation kinetics in a thermally cycled bulk $Pd_{40}Ni_{40}P_{20}$ glass. J Alloys Compd, 2022, 915: 165386
37 Ye J C, Lu J, Liu C T, et al. Atomistic free-volume zones and inelastic deformation of metallic glasses. Nat Mater, 2010, 9: 619–623
38 Zhang L T, Qiao J C. Relaxation behavior of high-entropy bulk metallic glass: Influences of physical aging and cyclic loading (in Chinese). Sci Sin-Phys Mech Astron, 2021, 51: 086111
39 Zhang L T, Wang Y J, Yang Y, et al. Aging and rejuvenation during high-temperature deformation in a metallic glass. Sci China-Phys Mech Astron, 2022, 65: 106111
40 Xu H Y, Li M Z. Activation-relaxation technique study on β-relaxation in $La_{55}Ni_{20}Al_{25}$ and $Cu_{46}Zr_{46}Al_8$ metallic glasses. Intermetallics, 2018, 94: 10–16
41 Ngai K L, Capaccioli S. Relation between the activation energy of the Johari-Goldstein β relaxation and T_g of glass formers. Phys Rev E, 2004, 69: 031501
42 Yang X S, Wang Y J, Wang G Y, et al. Time, stress, and temperature-dependent deformation in nanostructured copper: Stress relaxation tests and simulations. Acta Mater, 2016, 108: 252–263
43 Lu T, Liu S L, Sun Y H, et al. A free-volume model for thermal expansion of metallic glass. Chin Phys Lett, 2022, 39: 036401
44 Stringe M, Rösner H, Wilde G. Evidence for strain and a structural reset in $Pd_{40}Ni_{40}P_{20}$ bulk metallic glass. J Appl Phys, 2022, 132: 105107
45 Sohrabi S, Sun B Y, Mahmoodan M, et al. Rejuvenation by compressive elasto-static loading: The role of static stress on a Zr-based metallic glass. J Alloys Compd, 2023, 933: 167715
46 Zhang Y, Zhao H, Yan Y Q, et al. Ultrasonic-assisted fabrication of metallic glass composites. J Non-Crystalline Solids, 2022, 597: 121894
47 Gong X, Wang X D, Xu T, et al. β-relaxation and crystallization behaviors in a pulse-current-thermoplastic-formed La-based bulk metallic glass. J Phys Chem B, 2021, 125: 657–664
48 Qiao J C, Pelletier J M, Casalini R. Relaxation of bulk metallic glasses studied by mechanical spectroscopy. J Phys Chem B, 2013, 117: 13658–13666
49 Zhang L T, Pelletier J M, Qiao J C. Dynamic mechanical behavior of $(La_{0.7}Ce_{0.3})_{65}Al_{10}Co_{25}$ bulk metallic glass: Influence of the physical

aging and heat treatment. J Alloys Compd, 2021, 869: 159271
50 Johnson W L, Samwer K. A universal criterion for plastic yielding of metallic glasses with a $(T/T_g)^{2/3}$ temperature dependence. Phys Rev Lett, 2005, 95: 195501
51 Spaepen F. A microscopic mechanism for steady state inhomogeneous flow in metallic glasses. Acta Metall, 1977, 25: 407–415
52 Qiao J C, Pelletier J M. Mechanical relaxation in a Zr-based bulk metallic glass: Analysis based on physical models. J Appl Phys, 2012, 112: 033518
53 Alvarez F, Alegra A, Colmenero J. Relationship between the time-domain Kohlrausch-Williams-Watts and frequency-domain Havriliak-Negami relaxation functions. Phys Rev B, 1991, 44: 7306–7312
54 Lü Y J, Guo C C, Huang H S, et al. Quantized aging mode in metallic glass-forming liquids. Acta Mater, 2021, 211: 116873
55 Xu Z R, Yang D S, Qiao J C, et al. Unified perspective on structural heterogeneity of a LaCe-based metallic glass from versatile dynamic stimuli. Intermetallics, 2020, 125: 106922
56 Zhai W, Wang C H, Qiao J C, et al. Distinctive slow β relaxation and structural heterogeneity in (LaCe)-based metallic glass. J Alloys Compd, 2018, 742: 536–541
57 Qiao J C, Pelletier J M. Kinetics of structural relaxation in bulk metallic glasses by mechanical spectroscopy: Determination of the stretching parameter β_{KWW}. Intermetallics, 2012, 28: 40–44
58 Wang Z, Sun B A, Bai H Y, et al. Evolution of hidden localized flow during glass-to-liquid transition in metallic glass. Nat Commun, 2014, 5: 5823